# Mobile Campimetry

Marcelo M. Oliveira[a,1], Luiza A. Hagemann[a,2], Airton L. Kronbauer[b,3], Manuel M. Oliveira[a,5]

[a] *Instituto de Informática – UFRGS – Porto Alegre, Brazil*
[b] *Cenro de Olhos Rio Grande do Sul – CORS – Porto Alegre, Brazil*

**Abstract**

Campimetry is an important test to detect and monitor central and peripheral ocular dysfunctions, which might indicate the existence of serious conditions such as glaucoma, or the occurrence of strokes or brain tumors. Commercially-available campimeters are expensive and lack portability. We present a portable, low-cost, easy-to-manufacture smartphone-based campimeter. We evaluated our prototype in a user-study, which has shown that its results are consistent with the ones obtained with the Humphrey Field Analyzer - HFA II-i campimeter, with a Pearson correlation coefficient above 0.98 for all sampling positions on the visual field. Moreover, its reproducibility is also comparable to the Humprey campimeter. Given its portability and low cost, our mobile campimeter provides a promising alternative for patient screening in schools and community health centers, as well as for visual evaluation of patients with mobility restrictions, for keeping

[1] mmoliveira@inf.ufrgs.br
[2] lahagemann@inf.ufrgs.br
[3] alkronbauer@hotmail.com
[4] oliveira@inf.ufrgs.br

track of the visual field at home, and for use in communities with limited access to medical services.

*Keywords:* Campimetry, Smartphone-based Campimeter, Visual Acuity, Vision Health.

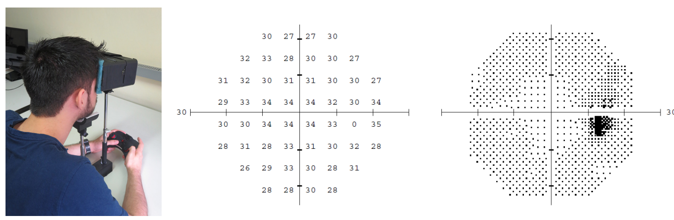


Figure 1: Our mobile campimeter. (left) Prototype during a visual field evaluation. (center) Minimum perceived intensities (in dB) computed by our campimenter and (right) its graphical representation (blind spot shown as a dark spot). A complete report example is shown in Appendix B.

## 1. Introduction

*Campimetry*, also known as *perimetry*, is an important test to detect and monitor central and peripheral ocular disfunctions. These might indicate the existence of serious conditions such as glaucoma, or the occurrence of strokes or brain tumors, which pose serious threats to one's health, and may dramatically affect the person's quality of life. Glaucoma, for instance, the leading cause of irreversible blindness, damages the optic nerve and often manifests itself as a silent disease. Without proper treatment, it may lend to blindness in just a few years [1]. Current estimates indicate that the worldwide prevalence of glaucoma in the population aged 40-80 years is approximately 3.54%, affecting over 64 million individuals, and should reach 76 million by

2020, and 111.8 million by 2040 [2]. Surprisingly, more than half of the patients suffering from glaucoma in developed countries are unaware of their condition. The situation is even more critical in underdeveloped countries.

Campimetry is a psychophysical test that checks the subject's perception of stimuli across the visual field. One eye at time, the patient should acknowledge each visual stimulus by pressing a button. The resulting maps reporting the minimum perceived intensities across the visual field are used by doctors along with other data (such as intraocular pressure or images of the optical nerve structure and the retina) for diagnosis.

The first concepts of computational campimetry appeared around 1970 [3] and provided the basis for current devices. Modern campimeters are still big and expensive, costing tens of thousands of dollars and found almost exclusively in ophthalmology clinics. Their lack of portability and high cost has prevented their widespread use as screening devices for ocular disfunctions. The availability of a portable, low-cost campimeter could change this situation, with the potential to significantly reduce the number of cases of avoidable blindness.

*We present a smartphone-based campimeter* designed to fulfill such needs. We have validated our prototype by performing a user study with 20 participants, who performed visual field evaluation both on our prototype and on a modern commercial campimeter (the Humprey Field Analyzer - HFA II-i). We compared the subjects' evaluations using statistical tools for perimetry examination [4], and show that the results produced by our prototype are consistent with the ones obtained with the HFA II-i campimeter, with a Pearson correlation coefficient above 0.98 for all sampling points on the visual field. Moreover, its reproducibility is also comparable to the one of the HFA II-i using the SITA Fast algorithm. Thus, our mobile campimeter provides a promising alternative for patient screening in schools, organizations, and communities with limited access to medical services, as well as for visual evaluation of patients with reduced mobility. Fig. 1 illustrates the use of our mobile campimeter prototype in one of its possible configurations, and shows examples of its reports.

The **contributions** of our work include:

- The design and demonstration of a portable, low-cost, smartphone-based campimeter (Section 3). Our prototype obtains results comparable to the ones obtained with commercial perimeters. Unlike these, ours does not require a controlled-lighting environment. The results of the exams can be sent to doctors and patients by instant messaging or making them available on-line;

- The design of optics and interactive software that allows a small programmable display at close proximity to the eye to be effectively used for visual-field evaluation (Section 3). Our solution is the first truly portable campimeter. Unlike commercially-available perimeters, ours contains no mechanically moving parts;

- A fast algorithm for visual field evaluation that obtains results comparable to the ones used in commercially-available campimeters, both in terms of quality and examination time (Section 3.3).

## 2. Background and Related Work

Some of the first methods used to evaluate the visual field were the Amsler Grid and the tangent screen [5, 6]. The first perimeter using a cupola shape, as used by commercial devices today, was designed by Goldmann in 1945. Fankhauser developed the first prototype of an automated perimeter in 1972 [3]. Since then, more sophisticated and precise devices and algorithms have been developed.

A modern campimeter works by projecting a series of white light stimuli of various intensities (brightness) across a uniformly illuminated cupola (background) that covers the patient's field of view. Covering one eye at a time with an eye patch, the patient looks at a central fixation point and indicates (by pressing a button) whether each stimulus is perceived. The goal of the exam is to determine the minimum perceived intensities at a set of sampling positions across the visual field. The estimated values are presented in decibels (dB), computed relatively to the intensity of the uniformly illuminated background.

Commercial perimeters are very similar both in shape and functionality. Currently, some of the most popular campimeters in the market are the Humphrey Field Analyzer (HFA) II-i series, manufactured by Zeiss [7], and the Octopus 900, manufactured by Haag-Streit [8]. They consist of a computer together with a mechanical, an electronic, and an optical sub-systems, making them heavy, big, expensive machines. For instance, the HFA II-i weights 40 Kg, occupying a volume of $60 \times 58 \times 51$ cm$^3$ [9], and costing tens of thousands of dollars. Carvalho et al. [10] have developed an automated campimeter with features similar to the commercially-available campimeters.

All these devices require a controlled-lighting environment for operation. In contrast, our mobile campimeter provides a truly portable, low-cost alternative for visual-field evaluation. Our co-design of optics and interactive software allows the use of a programmable display at close proximity, avoiding the need for controlled-lighting environment or mechanically moving parts.

Tafaj et al. [11] describe a PC-based solution inspired by a mechanical campimeter developed by Bruckmann et al. [12]. The evaluation of Tafaj et al.'s campimeter consisted in comparing its measurements of blind-spot sizes with the corresponding measurements obtained with an Octopus 101 perimeter. No evaluation of the minimum perceived intensities across the visual field has been provided [11].

In recent years, several works [13, 14, 15, 16] have evaluated the use of tablets (iPads) and apps to perform perimetry. In all these experiments, the tablet was kept at approximately 33 centimeters from the subject. During the test, the distance and positioning of the subject with respect to the device are checked by the tester through visual inspection. The use of tablets required a controlled-lighting environment and the tests were restricted to up to eight intensity values. Except for [13], these experiments used fixation points at the tablet's border, restricting the portion of the visual field that could be tested at once.

### *2.1. Head-Mounted-Display-based Solutions*

Matsumoto et al. [17] and Dariusz et al. [18] developed customized head-mounted displays (HMDs) for evaluating the visual field. Both HMDs use high-definition LCD displays and include additional hardware to provide eye-tracking. The equipment described by Matsumoto et al. [17] includes a sophisticated optical system consisting of several components. In both devices, the field evaluation is controlled by external processing units. Matsumoto et al. use a tablet to control the test and collect the patient's responses. The equipment described by Dariusz et al. is connected by cable to a personal computer through some customized hardware interface. Unlike these devices, our mobile campimeter uses a smartphone to control the field evaluation and collect the patient's responses, providing a low-cost, autonomous, portable solution.

### *2.2. Smartphone-based Eye Care Solutions*

Some researchers have proposed eye-care solutions based on smartphones. NETRA [19] describes an interactive solution for estimating refractive errors of the human eye (*e.g.*, myopia, hyperopia, and astigmatism). CATRA [20] provides a system for measuring and mapping cataracts. D-EYE [21] uses the smartphone camera and light source to allow retinal screening. The Portable Eye Examination Kit (PEEK) [22] uses apps to identify individuals with visual impairment. While these projects share several goals with ours (*e.g.*, portability, low cost, and potential to reach remote and underprivileged regions of the globe), we focus on campimetry, another important exam.

### *2.3. Algorithms*

Campimetry requires sampling the patient's field of view. Given the nature of the test, the patient's responses need to be double-checked to avoid incorrect feedback due to distraction or fatigue. This tends to make the test longer and, in turn, prone to more errors. Thus, a fast and reliable sampling strategy is highly desirable. SITA Fast [23] is the most popular algorithm used in commercial campimeters. It uses a simple staircase strategy, but its performance relies on the availability of a proprietary database containing statistical data about the population collected in previous exams over the years. Our field-of-view sampling algorithm (Section 3.3), although not based on a large database, has performance similar to the ones used by commercial campimeters.

## 3. Mobile Campimeter Design

Similar to commercial perimeters, our mobile campimeter estimates the minimum intensity visible by the patient at a set of sampling positions across the visual field. It consists of a virtual-reality-like headset driven by a smartphone. The psychophysical test is performed through an interactive app. The stimuli are presented (one at a time) on the smartphone's screen while the subject looks at a fixation point at the center of the field of view for the tested eye. During the test, an eye patch keeps the other eye closed. Next, we present the details of the hardware and software components of our mobile campimeter. We start by introducing a sampling grid (Section 3.1) for assessing the sensitivity of one's visual field to luminous stimuli. Section 3.2 discusses the hardware design and the associated goals and constraints that shaped our decisions. Our algorithm for evaluating the minimum perceived intensities across the patient's visual field is presented in Section 3.3. Section 3.4 describes how the results obtained with our mobile campimeter are scaled to the same decibel range used by commercial perimeters.

### *3.1. The Sampling Grid*

The grid of sampling positions (white dots) and the fixation point are shown in Fig. 2 (top). The fixation point is displayed as a red dot and kept on for the entire evaluation. During a visual field evaluation, the stimulus at each sampling position is rendered as a small circle of radius 2 pixels, using OpenGL ES [24] point primitive (`GL_POINT` with `glPointSize(2.0)` and `glEnable(GL_POINT_SMOOTH)`). Given the field of view covered by the smartphone screen (see Sec 3.2 - Headset Design), this corresponds to a 0.43 degree Goldmann size III stimulus, which is the standard size used in automated perimetry [25]. The background intensity of our current prototype corresponds to 18% of the maximum intensity of the smartphone. Although this value was chosen empirically, the Zone System in photography and some tone mapping algorithms often map middle-gray to 18% of the available dynamic range [26]. For each stimulus, the subject indicates whether it has been perceived by pressing a button on a bluetooth device (*e.g.*, a gamepad or a remote control - Fig. 3(f)) paired to the smartphone.

### *3.2. Hardware Design*

The hardware development included photometric measurements and the headset design. The first consisted in converting the absolute stimulus intensities displayed by the smartphone's screen to the luminance units used by commercial campimeters. The second describes the headset dimensions and optical system. The smartphone used in our prototype is a Samsung Galaxy S III running Android (Fig. 2).

**Photometric Measurements**: The intensity $d_c$ of a pixel in the smart-

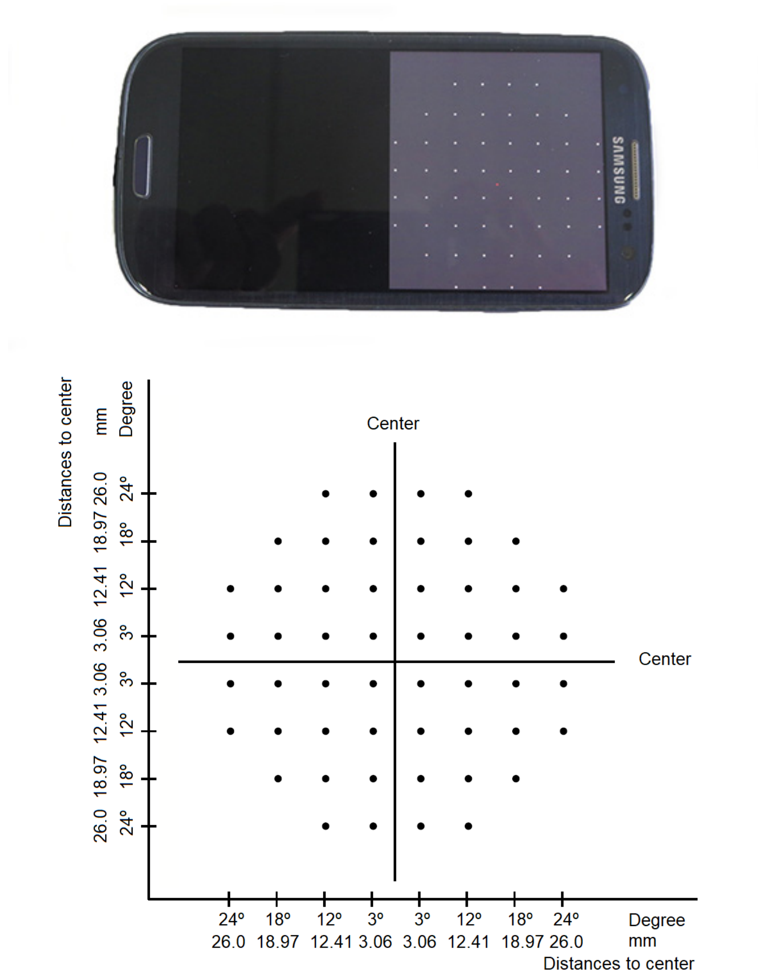


Figure 2: Smartphone (Samsung Galaxy S III) showing the grid of sampling positions (white dots) that cover the field of view for the right eye. The left eye is similar. The fixation point is shown as a red dot at the center of the field. The grid will appear centered to the patient when seen through the headset. The background intensity for the tested eye corresponds to 18% of the display's maximum intensity - compare it to the left part of the display. (bottom) Horizontal and vertical angles and coordinates associated with the sampling positions, expressed with respect to the fixation point.

phone's screen is specified in the normalized range $0 \leqslant d_c \leqslant 1$. Commercial campimenters adopt *apostilb* ($asb$) as their unit of luminance. For compatibility and to allow direct comparison of our results with the ones obtained with commercial devices, we convert the $[0, 1]$ $d_c$ range to apostilbs. To obtain such a conversion, we first measured the illuminance (expressed in *lux*, $lx = lm/m^2$) produced by the smartphone's screen for one hundred $d_c$ intensity values (uniformly sampled at 0.01 intervals) using a Minipa MLM-1020 luximeter [27]. We then converted the obtained lux values to apostilbs. The details of this conversion process are presented in Appendix A.

The background intensity on Humphrey perimeters is 31.5 asb or 10.0 $cd/m^2$. For our near-eye prototype, we used a background intensity of 3.45 asb or 1.01 $cd/m^2$.

**Headset Design**: Although loss of visual field due to glaucoma can occur anywhere in the visual field, in most patients detectable loss can be found in the 24-30° from the center [28]. Typically, evaluations performed by commercially-available campimeters cover approximately 48 degrees in the central field of view of each eye (*e.g.*, the HFA II-i evaluates 24 degrees temporally and 30 degrees nasally, for a total of 54 degrees). Other angular ranges are used only when some anomaly is detected in this test [25]. Our goal is to produce a smartphone-based compact device that covers 48 degrees in the central field of view, horizontally and vertically, for both eyes.

The screen of the smartphone used in our prototype is approximately 10.8 cm wide, and half of it should cover each eye (Fig. 2). Thus, the distance between the most external sampling position and the fixation point is approximately 2.6 cm. To subtend an angle of 48° for each eye, the dis-

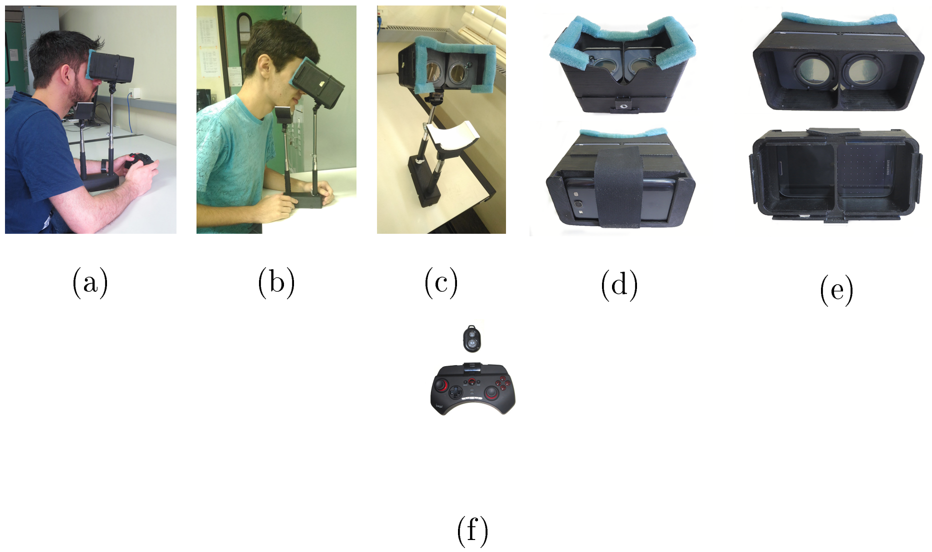


Figure 3: Our mobile campimeter and its components. (a-b) Prototype during a visual field evaluation. The adjustable support for the headset and chin lends to comfortable experiences by different subjects. (c) A view of the prototype with telescopic supports. (d) External views of the prototype: front (top) and back (bottom). (e) Internal views: lenses (top) and smartphone screen (bottom). (f) Bluetooth devices.

tance between the eye to the smartphone's screen (the object) should be $d = \frac{2.6}{\tan(24°)} \approx 5.84$ cm.

The closest distance onto which an (average) individual with normal vision is able to focus is 25 cm [29]. This distance is called the *near point* (aka *distance of most distinct vision*). Thus, we use a magnifier (*i.e.*, a positive lens) to allow the observer to focus on a virtual image of the smartphone's screen [29]. Note that this would preserve the 48° field of view, despite of the resulting magnification. The actual distance from the smartphone's screen to the optical system in our current 3D-printed prototype is $d = 6.50$ cm. The focal distance $f$ for a magnifier at distance $d$ from the object is given by [29]:

$$\frac{1}{f} = \frac{1}{d} - \frac{1}{25}, \tag{1}$$

where 25 cm is the near point. For $d = 6.50$ cm, this implies a magnifier with 11.4 diopters ($f \approx 8.78$ cm). Since the highest optical power that our lens manufacturer could produce for an aspherical lens was 10.0 diopters, we built an aspherical optical system consisting of two lenses: a 2 diopters lens ($f_1 = 50$ cm) in front of a 10 diopters one ($f_2 = 10$ cm), spaced by $s = 0.5$ cm. The effective focal distance $f'$ of the resulting optical system is given by [30]:

$$\frac{1}{f'} = \frac{1}{f_1} + \frac{1}{f_2} - \frac{s}{f_1 f_2}, \tag{2}$$

which results in an optical power of 11.9 diopters ($f' = 8.40$ cm). In a preliminary evaluation of our prototype, subjects reported that they could comfortably focus at the (virtual) image of the smartphone's screen.

Measured with respect to the fixation point, the sampling positions are at 3°, 12°, 18°, and 24° at both sides of the horizontal and vertical fields of view (*i.e.*, from -24° to 24°, at 6° intervals - Fig. 2 (bottom)). Since we use a flat screen, this translates into a non-uniform linear spacing among the sampling positions. Given the display-lens distance $d$ and considering the fixation point at the origin, the horizontal (vertical) coordinate of a sampling point making an angle of $\alpha$ degrees with the visual axis is given by $c = d \tan(\alpha)$. Thus, for the theoretical distance $d = 5.84$ cm and for angles of 3°, 12°, 18°, and 24°, the coordinates are respectively, 3.06 mm, 12.41 mm, 18.97 mm, and 26.00 mm away from the corresponding coordinate of the fixation point, both horizontally and vertically (Fig. 2 (bottom)). Since our current prototype has $d = 6.5$ cm, these sampling positions cover 21.8° instead of 24°. Improvements in the 3D printing and assembly of the prototype should remove such small discrepancy.

The headset was designed using the software SolidWorks [31] and produced on a 3D printer. It consists of two main parts: a frontal one, which contains the optical system (Fig. 3(e - top)); and a back part that houses the smartphone (Fig. 3(e - bottom)). The headset has a (removable) telescopic support for adjusting the height and orientation of the device to the patient-furniture arrangement. It also has an adjustable telescopic chin rest (Fig. 3(a)-(c)). Fig. 3 (a) and (b) show two individuals with different heights using our prototype. Note how the ability to adjust the heights of the telescopic supports as well as the orientation of the headset allows for customized experiences for different patients. Once detached from its support, the headset can be used by patients laying in beds. A bluetooth input device (Fig. 3(f)) paired to the smartphone is used to provide user feedback, informing that the current stimulus has been perceived by the patient. Some cushioning (blue sponge in Fig. 3) provides comfortable contact and helps to block ambient light.

### *3.3. Estimating the Minimum Perceived Intensities*

We have developed a binary-search-based algorithm for evaluating the minimum perceived intensities across the patient's visual field. In general, the minimum intensities perceived by an individual tend to be similar to the population-average minimum perceived values for the same positions. Our algorithm exploits this fact to accelerate convergence by starting the search near the population average. However, the actual result of the exam is not affected by the availability of such data. Similar to commercial campimeters, we also use the population-average values to position the patient with respect to the population results.

Let $F$ be the 2-D grid of sampling positions across the visual field (Fig. 2 and Fig. 4 (top left)). Given the left (or right) eye, its blind spot $b$ falls in a known neighborhood $B$ in $F$. During the evaluation of the visual field, the stimuli are randomly shown at positions across the grid $F$ for which the minimum intensities still need to be determined. The evaluation starts by detecting the blind spot. Thus, in the beginning of the examination, the chosen positions should alternate between inside and outside the neighborhood $B$ until the position of $b$ has been determined. The blind spot is defined as the grid position in $B$ with the largest number of patient misses. Once the position of the blind spot has been determined, the test proceeds until all positions in $F$ have their corresponding minimum perceived intensities estimated. The minimum intensity of a sampling position is determined when the difference between its maximum and minimum perceived intensities is less than a threshold (0.03 in the $[0, 1]$ $d_c$ range).

The minimum perceived intensity values vary across the visual field (Fig. 4 (left)). In order to quickly estimate the minimum perceived intensity at a sampling position $p_i$, we use a binary search. The initial intensity test value is set to $d_{ini} = 1.25 \times pm_i$ (converted to the smartphone's $[0, 1]$ intensity scale), where $pm_i$ is the population-average minimum perceived intensity at $p_i$. The lower boundary of the search interval is set to $d_{lower} = 0.19$, which is the first intensity above the background intensity ($d_{bkg} = 0.18$). The upper boundary is set to $d_{upper} = 1.0$. Given such initial and boundary values, the estimate of the minimum perceived intensity is obtained with the following procedure: if the patient perceives the stimulus with intensity $d_{ini}$, then the algorithm performs a binary search in the interval $[d_{lower}, d_{ini}]$; otherwise, it performs a binary search in the interval $[d_{ini}, d_{upper}]$. During the test, the system occasionally presents a stimulus at the location of the detected blind spot to double check if the patient has preserved the original head alignment.

The minimum reaction time for humans is 180 ms [32]. As such, we consider any patient's response below 180 ms as a false positive. Each stimulus is shown for 200 ms and the system waits additional 800 ms for the patient's answer. Thus, a new stimulus is shown every second. SITA Fast also uses a fixed time interval between consecutive stimuli [23, 32].

### *3.4. Dynamic Range*

The HFA II-i campimenter can generate light stimuli with brightness varying from 0.08 asb up to 10,000 asb [25]. Since such stimuli are projected onto a uniformly illuminated background, its full brightness range can, theoretically, be exploited. According to our measurements (Section 3.2 - Photometric Measurements), the brightness of the stimuli that can be displayed on the screen of the smartphone used to build our prototype varies from 0.13 asb up to 168.46 asb. Since its background intensity is set to 3.45 asb or 1.01 $cd/m^2$ (Fig. 2), the actual intensity range available for examination varies from 4.24 asb (1.35 $cd/m^2$) to 168.46 asb (53.62 $cd/m^2$). This corresponds to a maximum decibel value of $Max\_dB_{prot} = 10\log(168.46/4.24) \approx 16$ dB. The HFA II-i, in turn, can reach a maximum decibel value of $Max\_dB_{HFA} = 10\log(10,000/0.08) \approx 51$ dB. However, the upper 11 dB of the stimulus range (*i.e.*, from 41 to 51 dB) results from very dim stimuli, which fall beyond the range of human vision under standard testing conditions [25]. Thus, for practical purposes $Max\_dB_{HFA} = 40$ dB, which gives us a factor of $Max\_dB_{HFA}/Max\_dB_{prot} = 2.5$.

To produce reports that can be directly compared to the ones of commercial campimeters and allow doctors to interpreted them in the same way, we scale the dB values estimated with our prototype to the range of the HFA II-i. For this, we performed a simple experiment to estimate a per-sampling-position scaling factor. We had six volunteers to perform a field examination for each eye on both devices. Note that some of these volunteers did not take part in the user study described in Section 4. For each eye, and for each sampling grid position $p_i$, we computed a corresponding scaling factor $s_i$ as the average of the ratios of the corresponding values in the two exams for the same subject/eye (Eq. (3)):

$$s_i = \frac{1}{n}\sum_{j=1}^{n}(h_{ji}/m_{ji}), \tag{3}$$

where $h_{ji}$ and $m_{ji}$ are, respectively, the minimum intensity values (in dB) for the sampling position $p_i$ in the HFA II-i and in our mobile campimeter reports for the j-th subject. For the results shown in the paper, we used $n = 6$, although a larger number would be desirable, given the variability observed even when repeating the evaluation of a given subject/eye on the same device. Fig. 5 shows the estimated scaling factors for each visual-field sampling position on the right eye. Note that they are all close to the predicted 2.5 factor, with the largest values close to the blind spot. Fig. 4 (top) shows examples of reports generated by our prototype. The numbers are in decibels (dB), with the blind spot exhibiting a value of zero. In the graphical representation on the right, the blind spot is shown as a black region. For comparison, the corresponding reports produced by the HFA II-i for the same subject/eye are shown in Fig. 4 (bottom). An example of a complete report generated by our mobile campimeter is shown in Appendix B.

## 4. User Study and Results

To validate our mobile campimenter prototype and evaluate its performance relative to the Humphrey HFA II-i, we performed a user study involving a group of 20 volunteers with normal or corrected to normal vision. These included 17 males (ages 24 to 31), and 3 females (ages 23 to 27). Each subject performed two visual field examinations (test and retest) using both the Humphrey HFA II-i perimeter and our mobile campimeter prototype. This non-invasive user study was approved by the Federal University of Rio Grande do Sul (UFRGS) Medical Ethics Committee (document number 1.652.293). The HFA II-i perimeter used in this research is registered under number 10332030093 at the National Agency for Health Surveillance (ANVISA) in Brazil. The exams using the Humphrey perimeter were carried out at an ophthalmology center (CORS).

Some volunteers had their visual field evaluation performed first on the HFA II-i and then on our prototype, while the remaining had their evaluation first on the prototype and then on the HFA II-i. All volunteers had their examinations over a period of two days. In each day, two evaluations (test and retest) were done with the same device, with a twenty-minute interval between the tests. This way, the tests on a given device did not influence the results of tests on the other equipment. The retest was intended to check the repeatability of the evaluation on each device and to detect problems due to distractions during the evaluation. From a total of 40 evaluations, the average evaluation time was 2 minutes and 50 seconds on the HFA II-i using SITA Fast, and 3 minutes and 26 seconds on our prototype using the algorithm described in Section 3.3.

We performed a detailed analysis of the evaluation results. These include separate scores for each volunteer's eye in each device, comparison of the subjects' results obtained in both devices, and comparison of the subjects' results against the (estimated) population means. In each case, the comparisons considered the individual sampling positions across the visual field. For this analysis, we also use statistical indices proposed by [4], which include *mean deviation*, *pattern standard deviation* (Fig. 6), as well as a reproducibility evaluation (Fig. 8) based on the method by [33].

### *4.1. Mean Deviation*

The *mean deviation* (MD) index is a weighted average deviation from the normal reference field. It is used to detect regions in the visual field that present minimum intensity values significantly different from an average normal field. It is computed as

$$MD = (\frac{1}{N}\sum_{i=1}^{N}\frac{(v_i - \mu_i)}{{\sigma_i}^2})/(\frac{1}{N}\sum_{i=1}^{N}\frac{1}{{\sigma_i}^2}), \quad (4)$$

where $v_i$, $\mu_i$, and $\sigma_i^2$ are, respectively, the estimated minimum intensity value, the population minimum intensity average, and the population minimum intensity variance for sampling position $p_i$. $N$ is the number of sampling positions in the visual field, excluding the blind spot.

The graph on the left of Fig. 6 compares the mean deviation computed for our prototype and for the HFA II-i perimeter. The 40 points in the graph show the average of test and retest for 20 volunteers considering the left and the right eyes. Note that, although the average mean deviation is smaller for the HFA II-i, the values vary consistently in both devices: when the MD index computed for the HFA decreased/increased from one subject/eye to another, a similar variation was observed for the MD index computed for our prototype. The MD indexes shown in Fig. 6 (left) have a Pearson correlation coefficient of 0.754, indicating a strong agreement.

### *4.2. Pattern Standard Deviation*

The *pattern standard deviation* (PSD) index is the weighted standard deviation on each point between the measured intensity and the normal reference field. We check how far the measured value for this point is from its average and from the mean deviation. A small PSD value indicates that the measured values are close to the normal reference field, whereas a big PSD value indicates one or more regions with a big difference to the normal reference field. The PSD index is computed with Eq. (5). The graph on the right of Fig. 6 compares the PSD values computed for our prototype and for the HFA II-i perimeter, considering the evaluations performed in the user study. The Pearson correlation coefficient for the values in the two curves is 0.4, indicating a weak-to-moderate agreement.

$$PSD^2 = \frac{1}{N}\sum_{i=1}^{N}{\sigma_i}^2 \frac{1}{N-1}\sum_{i=1}^{N}\frac{(v_i - \mu_i - MD)^2}{{\sigma_i}^2}. \tag{5}$$

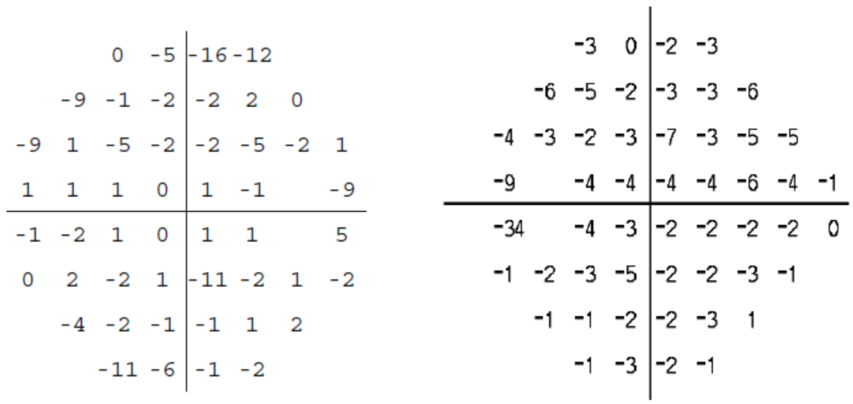


Figure 7: Mean deviation values for field evaluations with high PSD values performed with (left) HFA II-i and (right) Our prototype.

Fig. 7 shows the mean deviation values for field examinations with high PSD values obtained with our prototype (left) and with the HFA II-i (right). For the case of our prototype, the high mean deviation values are likely due to occlusions of sampling points close to the border of the visual field, as a result of an eye-headset misalignment.

### *4.3. Reproducibility*

The reproducibility analysis considers the root mean square error between the test and retest for a given subject/eye on the same device:

$$RMSE = \sqrt{\frac{1}{N}\sum_{i=1}^{N}(v_{i1} - v_{i2})^2}, \tag{6}$$

where $v_{i1}$ and $v_{i2}$ are the minimum intensity values associated with sampling position $p_i$ for the test and retest, respectively. The error should be close to zero if test and retest are consistent. Fig. 8 shows that the behavior of the curves in both devices is similar in most cases. On average, the RMSE for the prototype is slightly smaller than the one for the HFA II-i: 2.16 dB for the prototype and 2.38 dB for the HFA II. Appendix B provides a detailed comparison of the results for the test and retest for each subject/eye on both devices.

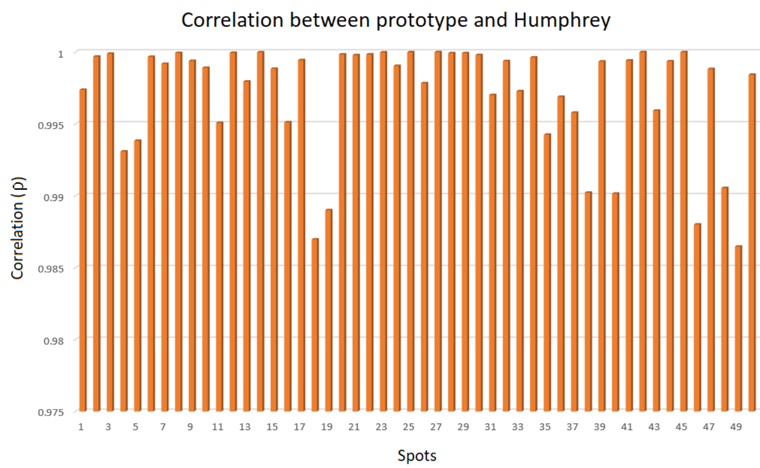


Figure 9: Pearson correlation coefficient $\rho$ between the minimum intensity values estimated by our prototype and the HFA II-i for each of the 50 sampling positions in the visual field.

### *4.4. Pearson Correlation between Devices*

We computed the Pearson correlation coefficient $\rho$ between the minimum intensity values estimated by our prototype and by the HFA II-i for each of the 50 sampling positions in the visual field (Fig. 9). The results show a very strong correlation, with $\rho > 0.98$ for all sampling positions.

### *4.5. Discussion*

Campimetry is an exam that requires the patient's total attention for a few minutes. Thus, it is important to allow her/him to be comfortable during the examination, avoiding lack of attention due to tiredness. For this, we have designed our mobile campimeter with adjustable supports for the headset and for the chin (Figures3 (a-b)). While a large variety of virtual-reality glasses are available on the market, they were designed for a different purpose, and do not provide this kind of feature. Moreover, to use the full display resolution for the desired field-of-view (48° per eye), we designed a headset with a bigger distance from its optical system to the smartphone screen (approximately 2 cm longer) than the typical distance found in commercially available virtual-reality glasses. Designing our own headset gave us more flexibility in our project decisions.

For our current prototype, we divided the smartphone's canonical ([0,1]) intensity interval into 100 steps of 0.01. As the device's maximum intensity increases, the size of the quantization step can be reduced, making the measurements more precise. However, since it is unlikely that the dynamic range of smartphones matches the one of commercial campimeters anytime soon, a scaling procedure such as the one described in Section 3.4 should still be required.

The use of an eye tracker could help to detect the situations in which the patient is looking away from the fixation point. This, however, has implications in terms of cost and size, and is hard to integrate with a smartphone. Like most commercial devices, we avoid the need for an eye tracker by periodically testing the blind spot location.

The calibration measurements (see Appendix A) used disks (of variable radii) shown under the luximeter's sensor. As a small disk moves away from the fixation point, one should expect an intensity falloff by the cosine of the angle ∠ABC formed by the fixation point (A), the eye position (B), and the center of the grid point (C) where the disk is located. For a centered 48° field-of-view, the maximum angle of a ray with the viewing direction is 24°, whose cosine is 0.913. Thus, the maximum intensity loss is under 10% and did not seem to have had any relevant impact on the visual field evaluation.

Our current prototype has a fixed interpupillary distance - IPD (6.2 cm). This decision was intended to simplify the design and construction of the prototype. However, this does not seem to affect the actual visual field examination, as perimetry is performed with a single eye opened at a time.

We emphasize that the goal of our mobile campimenter is not to replace commercial devices or ophthalmologists. It provides a portable and accessible alternative for screening patients, identifying the ones who need more careful examination, with the potential to reach remote and underprivileged areas.

### *4.6. Limitations*

The lenses used in our prototype have a diameter of 37.5 mm, causing the patient to look at the smartphone's screen through a circular window with a 34-millimeter diameter. Misalignments of the patient's eye with respect to such a window may happen during the evaluation, lending to occlusion of sampling points located at the borders of the visual field, affecting the estimated minimum intensity values at such positions. Fig. 10 illustrates this situation for one of the exams in our user study. Note the existence of two adjacent sampling positions with 0 dB values. The occurrence of such an outlier (a *double blind spot*) in healthy subjects results from an improper positioning of the eye with respect to the headset.

## 5. Conclusion

We have demonstrated a portable, low-cost, easy-to-manufacture smartphone-based campimeter. We evaluated our prototype through a user study and compared its results against the ones obtained on a Humphrey HFA II-i, one of the most popular commercially-available perimeters. We have presented detailed comparisons between both devices using several statistical indices. Our analyses have shown that the results obtained with our prototype are consistent with the ones obtained with the HFA II-i campimeter, with a Pearson's correlation coefficient above 0.98 for all sampling positions in the visual field. Moreover, its reproducibility and examination time are also comparable to the ones of the Humprey campimeter using the SITA Fast algorithm. Despite the use of modest hardware, our results exhibit good approximation to the ones obtained with commercial devices that cost tens of thousands of dollars. Given its true portability and low cost, our mobile campimeter provides a promising alternative for patient screening in schools and community health centers, as well as for visual evaluation of patients with mobility restrictions, for keeping track of the visual field at home, and for use in communities with limited access to medical services. The results of the exams can be sent to doctors and patients by instant messaging or made available on the Internet.

As future work, we would like to improve the design of our headset to reduce positioning misalignments, and use larger lenses to reduce occlusions of sampling positions at the border of the visual field.

## Acknowledgments

This work was sponsored by CNPq-Brazil (grants and fellowships 423673/2016-5, 306196/2014-0) and CAPES.

## Appendix A. Conversion of Measured Lux Values do Asb

To perform the measurements, we built a black box (its interior covered with black dull paint) to contain the smartphone at its bottom. The black box has a circular hole on top for the luximeter's sensor, isolating it from external light (Figure A.11 (left)). The sensor is located at a distance $r$ from the smarthphone's display (we used $r = 8$ cm). Since $1\,lx = 1\,sr\,cd/m^2$, and $3.14\ asb = 1\ cd/m^2$, we obtain

$$1\ asb = \frac{1}{3.14}\frac{lx}{sr}, \tag{A.1}$$

where $sr$ (steredian) is a measure of solid angle. Table A.1 shows the values (in lux) measured by the luximeter for ten $d_c$ intensities when displaying circles with radius ranging 5 to 30 mm.

The solid angle $\omega$ subtended by a circle with radius $R = MP$ displayed on the smartphone's screen is obtained as $\omega = A/r^2$, where $A$ is the area of the purple spherical cap shown in Fig. A.11 (right) and $r$ is the distance from the center of the sensor to the screen. The area $A$ of the spherical cap is given by $A = 2\pi rh$, where $h$ is the height of the spherical cap. By similar triangles (see Fig. A.11 (right)), $\frac{MP}{r} = \frac{a}{r-h}$. Thus, $h = r\left(1 - \frac{a}{MP}\right)$.

Since $a = \frac{MP}{OP}r$ and $OP = \sqrt{(R^2 + r^2)}$, $\omega = 2\pi\left(1 - \frac{r}{\sqrt{(R^2+r^2)}}\right)$. Thus, according to Eq. (A.1), given $v_L$, the value in lux measured by the luximeter

Table A.1: Illuminance (in lux) measured by the luximeter for 10 equally-spaced $d_c$ values and six circular stimulus with radius $R$ equal to 5, 10, 15, 20, 25, e 30 millimeters.

| $d_c$ | $R = 5$ | $R = 10$ | $R = 15$ | $R = 20$ | $R = 25$ | $R = 30$ |
|---|---|---|---|---|---|---|
| 0.1 | 0 | 0.11 | 0.19 | 0.26 | 0.38 | 0.49 |
| 0.2 | 0.22 | 0.68 | 1.44 | 2.39 | 3.57 | 4.78 |
| 0.3 | 0.45 | 1.63 | 3.49 | 5.92 | 8.77 | 11.81 |
| 0.4 | 0.83 | 3.11 | 6.68 | 11.2 | 16.6 | 22.8 |
| 0.5 | 1.33 | 4.90 | 10.45 | 17.7 | 26.4 | 35.6 |
| 0.6 | 1.97 | 7.52 | 16.07 | 27.5 | 40.5 | 54.4 |
| 0.7 | 2.81 | 10.64 | 23.1 | 39.1 | 57.4 | 76.6 |
| 0.8 | 3.83 | 14.51 | 31.6 | 53.0 | 77.6 | 103.4 |
| 0.9 | 5.01 | 19.00 | 41.3 | 69.1 | 100.9 | 132.5 |
| 1 | 6.34 | 20.6 | 52.5 | 87.9 | 129.1 | 161.3 |

for a circle with radius $R$ subtending a solid angle $\omega$ on the sensor, the value $v_A$ in apostilbs is given by

$$v_A = \frac{1}{3.14} \frac{v_L}{\omega}. \tag{A.2}$$

## Appendix B. Analysis of Test and Retest Results

This appendix provides detailed comparisons of the results for the test and retest for each subject/eye on both devices. Fig. B.12 compares the RMS error (Eq. (6)) in dB between test and re-test results for each subject/eye.

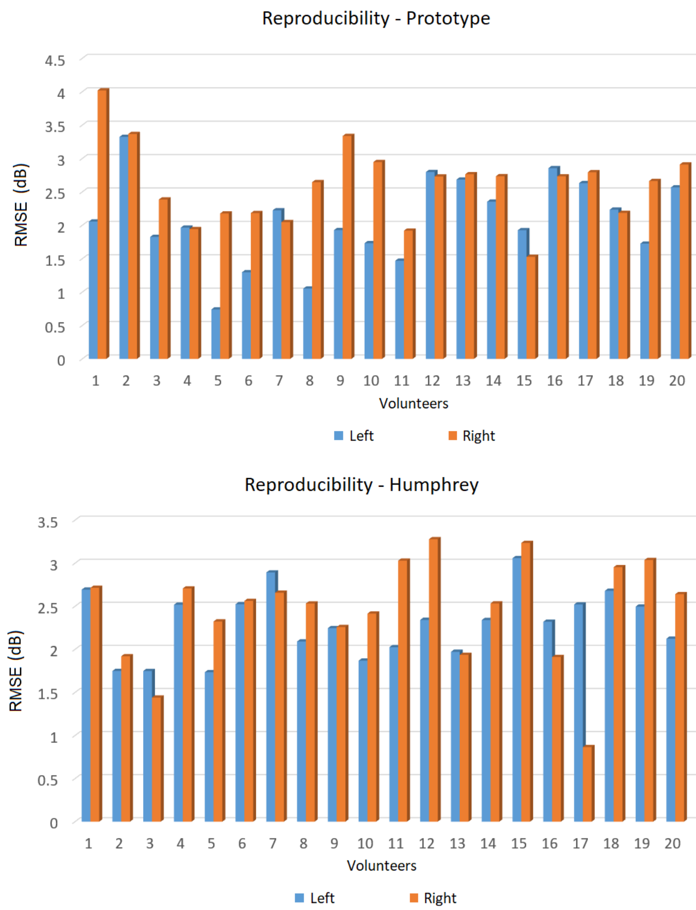


Figure B.12: Reproducibility: RMS error (Eq. (6)) in dB between test and re-test results for each subject/eye. (top) Our prototype. (bottom) HFA II-i.

Fig. B.13 compares mean deviation indices (Eq. (4)) in dB between test and re-test results for each subject/eye.

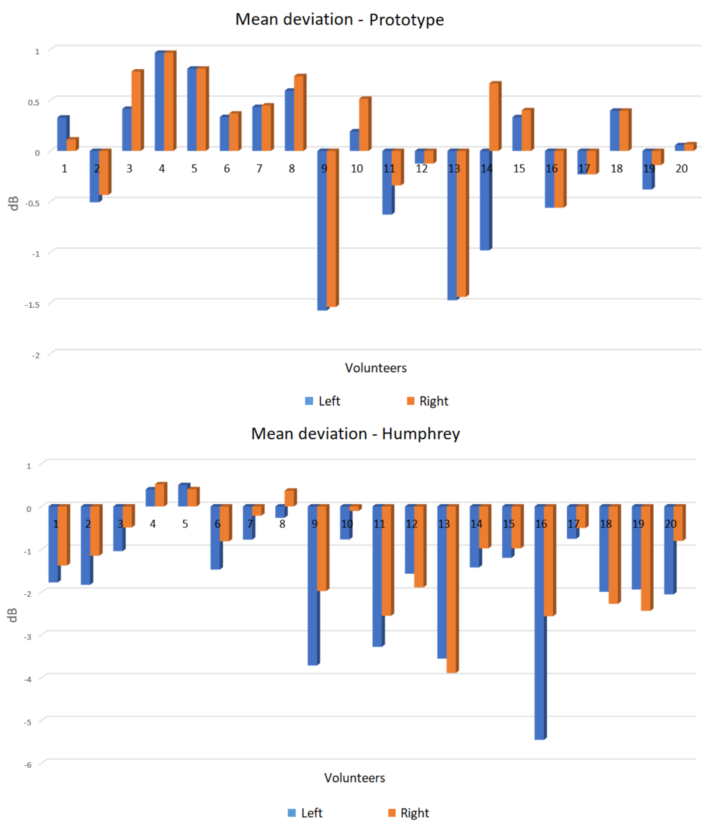


Figure B.13: Mean Deviation computed according to Eq. (4) considering test and re-test results for subject/eye. (top) Our prototype. (bottom) HFA II-i.

Fig. B.14 compares the pattern standard deviation indices (Eq. (5)) in dB between test and re-test results for each subject/eye.


Figure B.14: Pattern Standard Deviation computed according to Eq. (5) considering test and re-test results for each subject/eye. (top) Our prototype. (bottom) HFA II-i.

# Appendix C. Example of a Complete Evaluation Report

Figure C.15 shows an example of a complete evaluation report generated by our mobile campimeter. The reports are generated automatically at the end of each examination and saved as a PDF file in the smartphone storage.

## References


[1] Schacknow, P, Samples, J. The Glaucoma Book: A Practical, Evidence-Based Approach to Patient Care. SpringerLink : Bücher; Springer New York; 2010. ISBN 9780387767000.

[2] Tham, YC, Li, X, Wong, TY, Quigley, HA, Aung, T, Cheng, CY. Global prevalence of glaucoma and projections of glaucoma burden through 2040. Ophthalmology 2014;121(11):2081 – 2090. doi:10.1016/j.ophtha.2014.05.013.

[3] Weijland, A, Fankhauser, F, Bebie, H, Flammer, J. Automated Perimetry: Visual Field Digest. 5 ed.; Haag-Streit AG; 2004.

[4] Heijl, A, Lindgren, G, Olsson, J. A package for the statistical analysis of visual fields 1987;49:153–168. doi:10.1007/978-94-009-3325-5_23.

[5] Campbell, W, DeJong, R. DeJong's the Neurologic Examination. No. pt. 327,N$^{o}$ 2005 in DeJong's the Neurologic Examination; Lippincott Williams & Wilkins; 2005. ISBN 9780781727679.

[6] Madge, S. Clinical Techniques in Ophthalmology. Elsevier/Churchill Livingstone; 2006. ISBN 9780443103049.

[7] "Zeiss", . "Humphrey Field Analyzer - HFA II-i Series."; 2017 (Last accessed December, 2017). http://www.zeiss.com/meditec/en_de/products---solutions/ophthalmology-optometry/glaucoma/diagnostics/perimetry/humphrey-hfa-ii-i.html.

[8] "Haag-Streit", . "Octopus 900."; 2017 (Last accessed December, 2017). http://www.haag-streit.com/product/perimetry/octopusr-900.html.

[9] "Zeiss", . "Humphrey Field Analyzer - HFA II-i Series. Technical data"; 2017 (Last accessed December, 2017). https://www.zeiss.com/meditec/int/products/ophthalmology-optometry/glaucoma/diagnostics/perimetry/humphrey-hfa-ii-i.html#technical-data.

[10] de Carvalho, LAV, Romão, AC, Tonissi, S, Carozelli, P, Steffani, M. Desenvolvimento de um instrumento automatizado para medida do campo visual do olho humano. Revista Brasileira de Engenharia Biomédica 2007;23(1):5–16.

[11] Tafaj, E, Uebber, C, Dietzsch, J, Schiefer, U, Bogdan, M, Rosenstiel, W. Mobile and fast detection of visual field defects for elderly drivers as a necessary input into driver assistance systems for mobility maintenance. In: GMM-Fachbericht Band 64, AmE 2010 - Automotive meets Electronics. 2010, p. 47–52.

[12] Bruckmann, A, Volpe, NJ, Paetzold, J, Vonthein, R, Schiefer, U. Comparison of advanced visual field defects measured with the tübingen mobile campimeter and the octopus 101 perimeter. European journal of ophthalmology 2010;20 1:149–57.

[13] Zhichao, W, H., GR, J., JC, K., GJ, N., AL, D., LC, et al. Measurement of retinal sensitivity on tablet devices in age-related mac-

ular degeneration. Translational Vision Science & Technology 2015;4(3). doi:10.1167/tvst.4.3.13.

[14] George, KYX, Mingguang, H, G., CJ, J., VA, Aung, T, Cheng, CY. A comparison of perimetric results from a tablet perimeter and humphrey field analyzer in glaucoma patients. Translational Vision Science & Technology 2016;5(6). doi:10.1167/tvst.5.6.2.

[15] Schulz, AM, Graham, EC, You, Y, Klistorner, A, Graham, SL. Performance of ipadâĂŘbased threshold perimetry in glaucoma and controls. Clinical & Experimental Ophthalmology 2017;doi:10.1111/ceo.13082.

[16] J., VA, K., HJ, Sheryl, L, Veera, S, Michael, T, William, W, et al. Validation of a tablet as a tangent perimeter. Translational Vision Science & Technology 2016;5(4). doi:10.1167/tvst.5.4.3.

[17] Chota, M, Sayaka, Y, Hiroki, N, Sonoko, T, Sachiko, O, Shinji, K, et al. Visual field testing with head-mounted perimeter âĂŸimoâĂŹ. PLOS ONE 2016;11(8):1–12. doi:10.1371/journal.pone.0161974.

[18] Dariusz, W, A., FB, Alfredo, S, Ghazal, V, Vikas, C. Testing of visual field with virtual reality goggles in manual and visual grasp modes. BioMed Research International 2014;doi:10.1155/2014/206082.

[19] Pamplona, VF, Mohan, A, Oliveira, MM, Raskar, R. NETRA: Interactive display for estimating refractive errors and focal range. ACM Trans Graph 2010;29(4).

[20] Pamplona, VF, Passos, EB, Zizka, J, Oliveira, MM, Lawson, E, Clua, E, et al. CATRA: Interactive measuring and modeling of cataracts. ACM Trans Graph 2011;30(4).

[21] "D-EYE", . "D-EYE Posterior"; 2017 (Last accessed December, 2017). `https://www.d-eyecare.com`.

[22] "PEEK", . "Vision and Health for Everyone"; 2017 (Last accessed December, 2017). `https://www.peekvision.org/`.

[23] Bengtsson, B, Olsson, J, Heijl, A, Rootzen, H. A new generation of algorithms for computerized threshold perimetry, sita. Acta Ophthalmologica Scandinavica 1997;75(4):368–375.

[24] Ginsburg, D, Purnomo, B, Shreiner, D, Munshi, A. OpenGL ES 3.0 Programming Guide. OpenGL; Pearson Education; 2014. ISBN 9780133440126.

[25] Heijl, A, Patella, VM, Bengtsson, B. Effective Perimetry: The Field Analyzer Primer. 4 ed.; Carl Zeiss Mediatec, Inc.; 2012.

[26] Reinhard, E, Stark, M, Shirley, P, Ferwerda, J. Photographic tone reproduction for digital images. ACM Trans Graph 2002;21(3):267–276.

[27] "Minipa", . "Minipa"; 2017 (Last accessed December, 2017). `http://www.minipa.com.br/temperatura-e-ambiente/luximetros/141-mlm-1020`.

[28] Ballon, BJ, Echelman, DA, Shields, MB, Ollie, AR. Peripheral visual field testing in glaucoma by automated kinetic perimetry with the

humphrey field analyzer. Archives of Ophthalmology 1992;110(12):1730–1732. doi:10.1001/archopht.1992.01080240070033.

[29] Jenkins, F, White, H. Fundamentals of Optics. International student edition; McGraw-Hill; 1976. ISBN 9780070323308.

[30] Hecht, E. Optics. 4th ed.; Addison-Wesley; 2002.

[31] Systemes", D. "Solidworks"; 2017 (Last accessed December, 2017). http://www.solidworks.com/.

[32] Olsson, J, Bengtsson, B, Heijl, A, Rootzen, H. An improved method to estimate frequency of false positive answers in computerized perimetry 1997;75(2):3–181.

[33] Bengtsson, B, Heijl, A. Sita fast, a new rapid perimetric threshold test. description of methods and evaluation in patients with manifest and suspect glaucoma. Acta Ophthalmologica Scandinavica 1998;76(4):431–437.

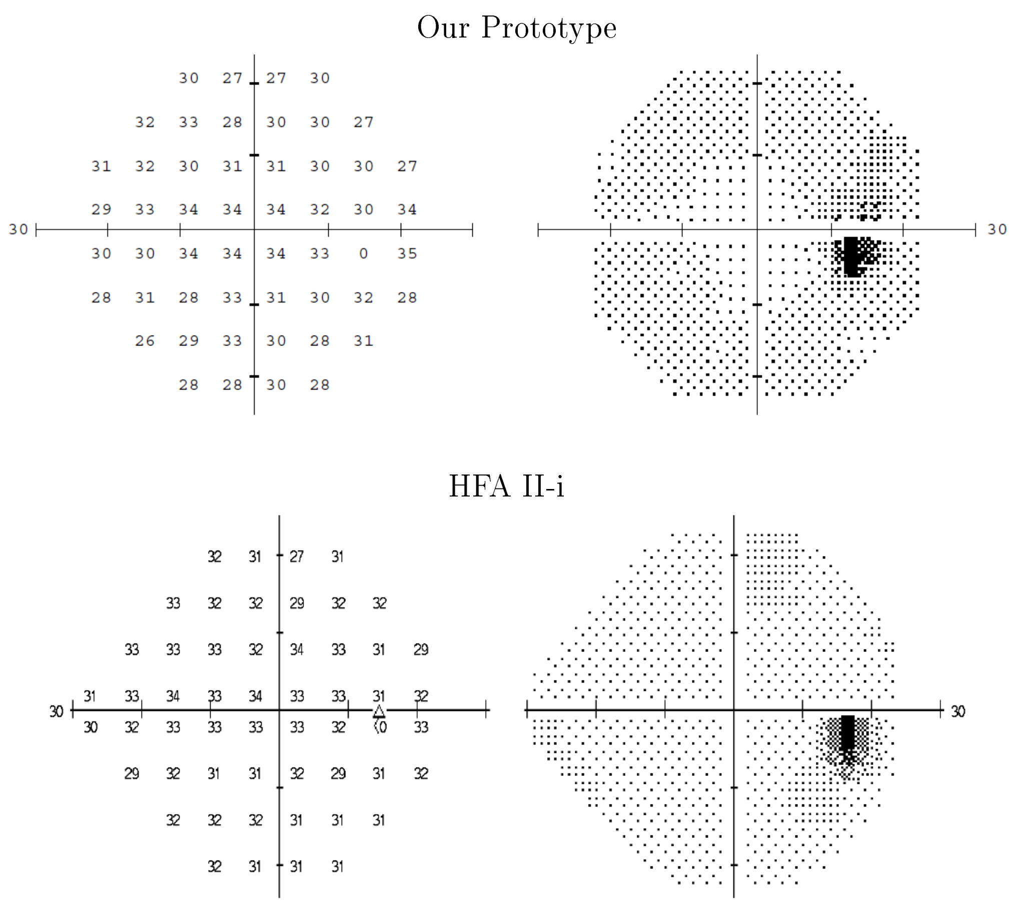


Figure 4: Campimetry reports produced by our prototype (top row) and by the Humphrey HFA II-i (bottom) for the same eye of a given patient. (left) Maps showing the minimum perceived intensity for each sampled point of the visual field, expressed in decibels (dB). (right) Graphical representations of the numerical maps on the left. In each report, the blind spot appears as a black region and corresponds to a value of 0 (zero) dB in the numerical map.

**Scaling Factors**

| | | | | | | | |
|---|---|---|---|---|---|---|---|
| | | 2.14 | 1.93 | 1.93 | 2.15 | | |
| | 2.29 | 2.38 | 2.21 | 2.31 | 2.31 | 2.08 | |
| 2.13 | 2.29 | 2.21 | 2.07 | 2.13 | 2.14 | 2.31 | 2.14 |
| 2.13 | 2.20 | 2.27 | 2.27 | 2.27 | 2.36 | 2.14 | 2.46 |
| 2.21 | 2.20 | 2.27 | 2.33 | 2.27 | 2.20 | | 2.54 |
| 2.15 | 2.38 | 2.21 | 2.20 | 2.13 | 2.14 | 2.36 | 2.00 |
| | 2.00 | 2.23 | 2.21 | 2.21 | 2.07 | 2.13 | |
| | | 2.00 | 2.07 | 2.14 | 2.00 | | |

Figure 5: Scaling factors computed with Eq. (3) for the right eye. They are used to adjust the dB values of the mininum perceived intensities estimated by our prototype to allow a direct comparison with the HFA II-i report.

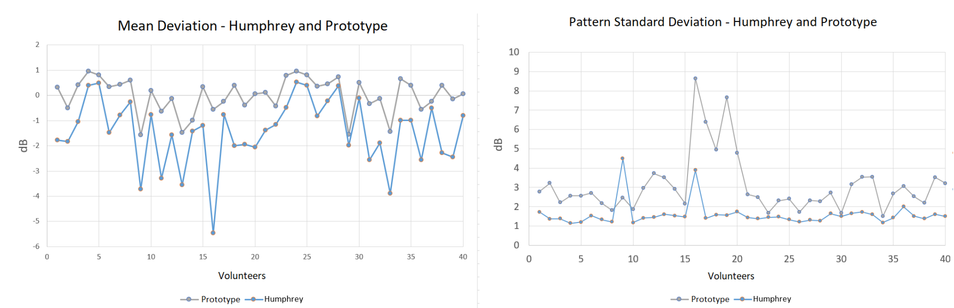


Figure 6: Comparisons between our prototype and the Humphrey perimeter. The 40 points in the graphs show the corresponding index values computed considering the average of test and retest for each eye, for 20 volunteers. (left) Mean deviation (MD). (right) Pattern standard deviation (PSD).

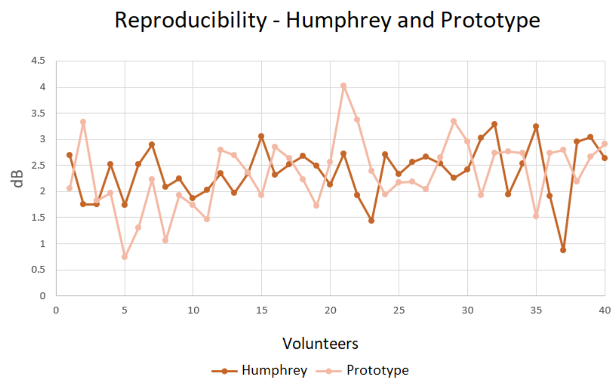


Figure 8: Comparison of the reproducibility between our prototype and the HFA computed as the root mean square error between test and retest for a given subject/eye on the same device.

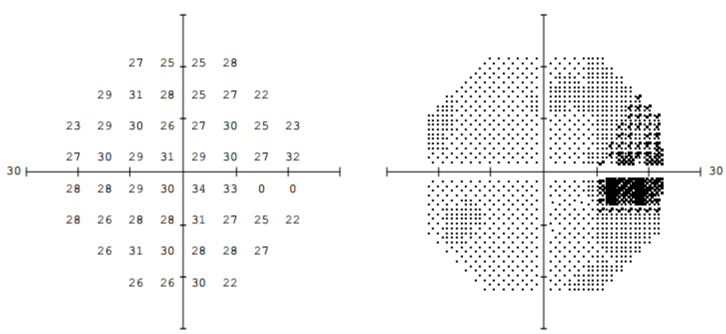


Figure 10: Misalignments of the patient's eye with respect to the headset may lend to occlusion of sampling points located at the borders of the visual field. This example shows a *double blind spot* resulting from misalignment.

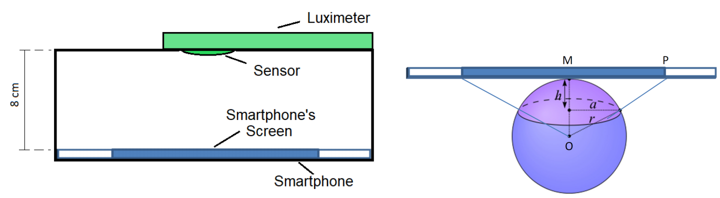


Figure A.11: Phometric measurement. (left) A black box with a circular hole on top for positioning the luximeter's sensor facing the smartphone's screen, placed at a distance $r$ $(= 8)$ cm away at the bottom of the box. The black box isolates the sensor from external light. (right) Geometric configuration for estimating the solid angle subtended by a circle of radius MP displayed on the smartphone's screen, as perceived by the luximeter's sensor. The sensor is located at the center of the sphere, at a distance $r$ from the smartphone screen. The solid angle subtended by the circle is obtained dividing the area of the purple spherical cap by $r^2$.

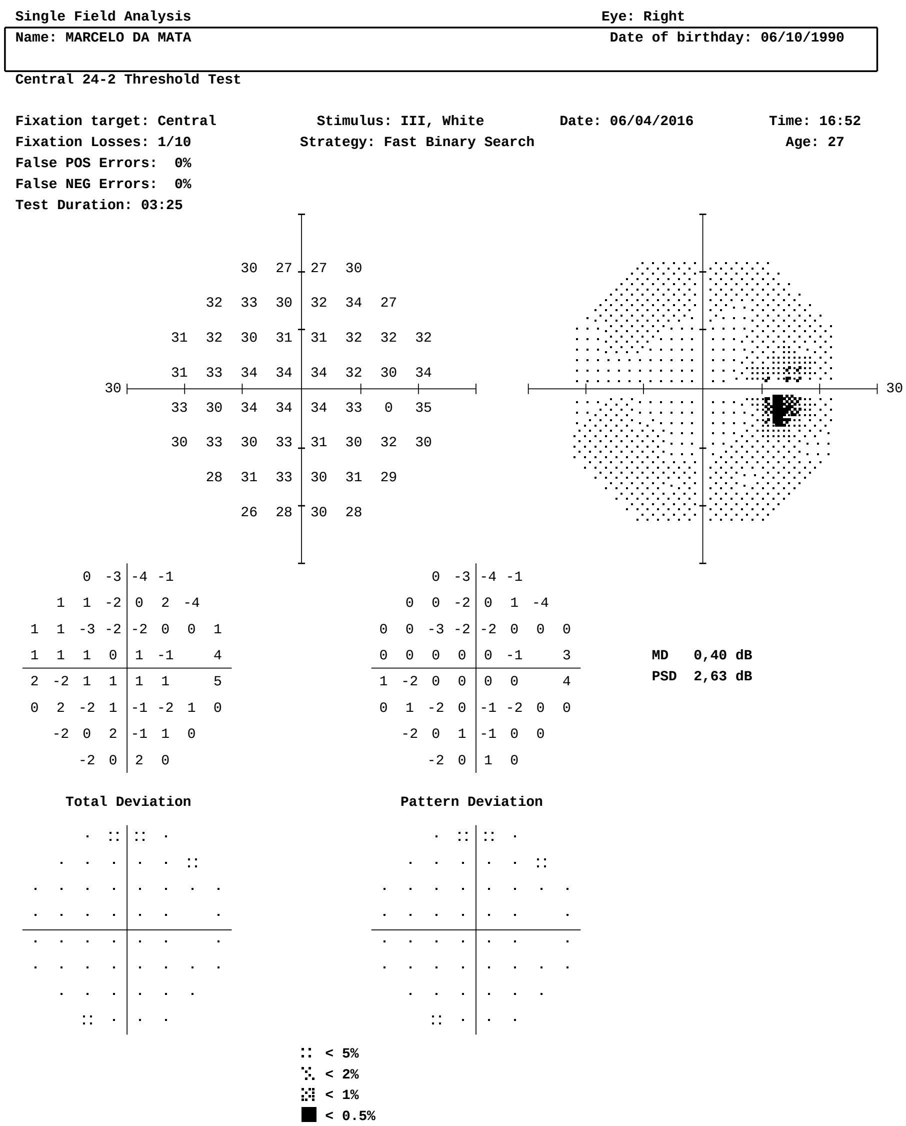


Figure C.15: Example of a full report generated by our mobile campimeter.